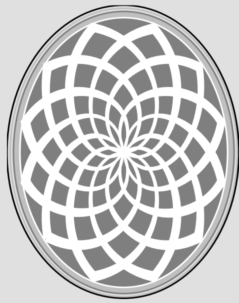

Interdisciplinary Mathematics Institute

2016:01

Development and Experimental Validation of a Model for Oral Multispecies Biofilm Recovery after Chlorhexidine Treatment

Ya Shen, Jia Zhao, César de la Fuente-Núñez, Zhejun Wang, Robert E. W. Hancock, Clive R. Roberts, Jingzhi Ma, Qi Wang and Markus Haapasalo

IMI

Preprint Series

College of Arts and Sciences
University of South Carolina

Development and Experimental Validation of a Model for Oral Multispecies Biofilm Recovery after Chlorhexidine Treatment

Ya Shen[1¤], Jia Zhao[2¤], César de la Fuente-Núñez[3,6], Zhejun Wang[1], Robert E. W. Hancock[3], Clive R. Roberts[4], Jingzhi Ma[5], Qi Wang[2]* and Markus Haapasalo[1]*

[1]Division of Endodontics, Department of Oral Biological and Medical Sciences, Faculty of Dentistry, University of British Columbia, Vancouver, British Columbia, Canada; [2]Department of Mathematics, University of South Carolina, Columbia, USA; [3]Centre for Microbial Diseases and Immunity Research, Department of Microbiology and Immunology, University of British Columbia, Vancouver, Canada; [4]Department of Oral Biological and Medical Sciences, Faculty of Dentistry, University of British Columbia, Vancouver, British Columbia, Canada; [5]Department of Stomatology, Tongji Hospital, Tongji Medical College, Huazhong University of Science and Technology, Wuhan, China; [6]Synthetic Biology Group, MIT Synthetic Biology Center, Research Laboratory of Electronics, Department of Biological Engineering, Department of Electrical Engineering and Computer Science, Massachusetts Institute of Technology, Cambridge, Massachusetts, United States of America. Broad Institute of MIT and Harvard University, Cambridge, Massachusetts, United States of America.

Short title: Biofilm resistance to chlorhexidine

[¤] These authors contributed equally to this work.

***Corresponding authors**:

qwang@math.sc.edu (Qi Wang)

Department of Mathematics, Interdisciplinary Mathematics Institute and NanoCenter at USC, University of South Carolina, Columbia, SC 29063, USA

markush@dentistry.ubc.ca (Markus Haapasalo)

Division of Endodontics, Oral Biological and Medical Sciences, UBC Faculty of Dentistry, 2199 Wesbrook Mall, Vancouver, BC, Canada V6T 1Z3

Author contributions

Conceived and designed the experiments: YS QW MH. Performed the experiments: YS JZ. Analyzed the data: YS JZ CDLF-N ZW. Contributed reagents/materials/analysis tools: YS JZ QW MH. Wrote the paper: YS JZ ZW CDLF-N REWH MH QW CRR JM.

Funding

This work was partly supported by Canada Foundation for Innovation (CFI fund, project number 32623), Canada. R.E.W.H. holds a Canada Research Chair in Microbiology and was funded through the Canadian Institutes for Health Research. C.D.L.F.-N. received a scholarship from the Fundación "la Caixa" and Fundación Canadá (Spain), and currently holds a postdoctoral scholarship from Fundación Ramón Areces (Spain). JZ was partially supported by a SPARC Graduate Research Fellowship from the Office of the Vice President for Research at the University of South Carolina. JZ and QW's research is partially supported by an NSF award DMS-0908330 and DMS-1200487. QW's research is also partially supported by an AFOSR's award FA9550-12-1-0178 and SC EPSCOR GEAR awards.

Competing Interests: The authors have declared that no competing interests exist.

Abstract

We combined experiments and mathematical modeling to study the recovery of oral multispecies biofilms following antimicrobial treatment, and further utilized mathematical modelling to explore the dynamics of the tolerance mechanisms of biofilms. Specifically, we investigated the proportion of viable bacteria in multispecies biofilms over time after exposure to chlorhexidine gluconate (CHX) or CHX with surface modifiers (CHX-Plus). The oral multispecies biofilms were grown for three weeks and then treated with 2% CHX or CHX-Plus for up to 10 minutes. Confocal laser scanning microscopy showed that CHX-Plus killed bacteria in biofilms more effectively than the regular 2% CHX. Cell death continued to increase for up to one week after exposure to the two CHX solutions. Two weeks after the CHX treatment, the biofilms had started to recover. Five weeks later, the proportion of the viable bacteria had recovered in the 1 and 3 minutes treatment groups but not after the 10 minutes treatment. The number of viable bacteria in all biofilms treated with the two CHX solutions returned to the pretreatment level eight weeks after exposure. To elucidate the mechanism, a new mathematical model for multiple bacterial phenotypes was developed to monitor the live and dead bacterial populations as well as the volume fraction of extracellular polymeric substances. The model adopted the notion that bacterial persisters exist in biofilm, which can survive CHX treatment. The model was then used to predict the viable bacterial population present after CHX treatment, which revealed the crucial role of not only by quorum sensing (QS) but also by persister cells in bringing about biofilm recovery. The present study indicates that the formation of recalcitrant oral biofilms probably leads to difficult-to-treat root canal infection, and provides insight into the kinetics of the bacterial persisters and the behavior of QS molecules in multispecies biofilms after antimicrobial treatment.

Introduction

Apical periodontitis is an inflammatory reaction of periradicular tissues caused by a microbial infection in the root canal [2]. Because the bacteria in the necrotic root canal system grow mostly in sessile biofilms, the success of endodontic treatment will depend to a great extent on the effective eradication of such biofilms [3]. Chemo-mechanical instrumentation has been regarded as the key element of endodontic treatment. Mechanical canal preparation supports disinfection by disturbing or detaching biofilms that adhere to canal surfaces and by removing a layer of infected dentin and creating space for disinfecting solutions. Anatomic complexities represent physical constraints that pose a challenge to adequate root canal disinfection. Several studies using advanced techniques such as microcomputed tomography scanning have demonstrated that proportionally large areas of the main root-canal wall remain untouched by the instruments [4], emphasizing the need for chemical means of cleaning and disinfecting all areas of the root canal. However, the available irrigants that exhibit direct antibacterial activity also face great challenges in eradicating root canal biofilms. The protective mechanisms underlying biofilm antimicrobial resistance are not yet fully understood, although several mechanisms have been proposed [5,6]. These mechanisms include physical or chemical diffusion barriers to antimicrobial penetration into the biofilm [7], slow growth of the biofilm due to nutrient limitation, altered gene expression of resistance genes due to activation of the general stress response and/or adaptation to growth on surfaces, and the emergence of a biofilm-specific phenotype [8].

Endodontic treatment does not always fully eradicate bacteria during infections, leading to interactions between the bacteria and the surrounding host tissues, thus compromising clearance of the infection. Persistent and recurrent apical periodontitis have been the focus of interest in endodontic research for a long time [9-12]. The primary cause of post-treatment apical periodontitis is acknowledged to be the continuing presence of bacteria within the root canal system [12-15]. Histopathological investigations found biofilm structures in the great majority (74%) of cases of post-treatment apical periodontitis [16]. Thus biofilms are strongly associated with persistent infection in the root canal.

Irrigation has a central role in endodontic treatment [17]. Several irrigating solutions have antimicrobial activity and can actively kill bacteria and yeasts when in direct contact with the microorganisms [18-20]. The cationic bisbiguanide N,N'1,6-hexanediyl-bis [N'-(4-chlorophenyl)(imidodicarbonimidic-diamide)] (chlorhexidine digluconate; CHX) is one of the most commonly used irrigant solutions in the clinic due to its antimicrobial properties. CHX is also the active ingredient in many commercially-available disinfectants and antiseptics. As CHX is cationic it interacts with the negatively charged bacterial cell surface and translocates to the cytoplasmic membrane where it damages the membrane barrier leading to cell death [17,21]. A 0.2% CHX solution is widely used as an antimicrobial agent to prevent biofilm growth on tooth surfaces. For the current study, we used much higher concentrations to evaluate the susceptibility of dental biofilms to this agent.

Mathematical modeling has emerged as a powerful tool for studying biofilm dynamics; it utilizes a set of experimentally identified or implicated mechanisms and sheds light on how these basic mechanisms can influence the formation and evolutionary dynamics of biofilms [22]. Mathematical models come in many forms ranging from simple empirical correlations to sophisticated mechanistic, physics-based and computationally intensive ones that can describe three-dimensional biofilm morphology and interaction with the environment [23-25]. Most biofilm models available today, however, capture only a small fraction of the complexities of the biofilm system since each is developed based on a set of idealistic mechanisms, which perhaps apply only to specific biofilm systems. Furthermore, none is able to explain well the dynamic process of oral multispecies biofilm during recovery after treatment with CHX. Therefore, there was a need to devise a new mathematical model to interpret experimental findings for multispecies biofilms.

Here we have integrated mathematical modeling with an experimental approach to explore the parameters influencing viability of bacteria in biofilms over time after being treated with CHX. Our mathematical model is based on a set of pertinent assumptions regarding biofilm tolerance mechanisms, including the existence of persister cells (which represent dormant bacteria in a population that resist the action of antimicrobial agents) [25] as well as a portion of bacteria that are susceptible to the antimicrobial agent, and the quorum sensing effect [26,27]. The model was then

tested using the well-controlled experiments, making it possible to model the transition between the susceptible and persister cells. In these experiments, we described the effects exerted over time on a multispecies oral biofilm of two preparations containing high levels of CHX. Confocal laser scanning microscopy (CLSM) using fluorescent indicators of membrane integrity (*Bac*Light LIVE/DEAD viability stain) was used to determine biofilm architecture and the proportion of viable bacterial cells within the biofilm. Subsequently, scanning electron microscopy (SEM) was used to visualize compromised bacterial cells resulting from the CHX treatment. The experimental data were then used to calibrate the mathematical model. With the calibrated model, we examined the survival of bacteria in biofilms over time after exposure to the CHX protocol, and predicted the populations of bacterial persisters, extracellular polymeric substances (EPS), and quorum sensing (QS) molecules.

Results

Experimental Results

Staining of cells using the LIVE/DEAD stain helped determine the proportion of live-to-dead cells in the biofilm over time. First, biofilms were grown for a period of three weeks and the ratio of live to dead cells was calculated. The mature biofilms were then treated for 1, 3 or 10 minutes with either 2% CHX or CHX-Plus (Fig. 1). Immediately after treatment, the viability profile of the biofilm population changed, demonstrating an increased number of dead cells (Fig. 1). This occurred in all groups, but was more pronounced in biofilms treated with 2% CHX for 10 minutes and CHX-Plus for 3 and 10 minutes. CHX-Plus showed higher levels of bactericidal activity at all exposure times compared to 2% CHX ($P < 0.001$; Fig. 1) and indeed treatment with CHX-Plus for 3 minutes resulted in greater bacterial cell killing than the treatment for 10 minutes using 2% CHX (Fig. 1). As expected, increasing the treatment time with CHX-plus from 3 to 10 minutes led to increased cell death. The use of a CHX inactivator, which contains L-α-Phosphatidylcholine (α-Lecithin) (Sigma, St. Louis, MO, USA), Tween 80 (Sigma, St. Louis, MO, USA) and distilled water, subsequent to CHX treatment had no significant effect on the viability of the bacterial population, indicating that viability changes were likely due to the exposure to, and likely uptake of, CHX during the short application period (Fig. 1). In addition, there were significant differences ($P < 0.001$) with regards to bacterial viability during the

recovery phases between the CHX and CHX-Plus irrigants ($P < 0.001$) and after different treatment times (1, 3 and 10 minutes). Cell death in the biofilms continued to increase for up to one week after exposure to the two CHX solutions ($P < 0.001$). Two weeks after the CHX treatment the biofilms had started to recover, as shown by the increase in the ratio of live to total (live+dead) cells (Fig. 1). After five weeks of recovery, the proportion of viable bacteria almost reached the pre-treatment levels in all groups (87-91%), but were somewhat less in the 10-minute treatment groups (CHX-Plus: 77%; 2% CHX: 85%) (Fig. 1). Eight weeks after the treatment, biofilms in all groups had returned to pre-treatment levels of bacterial viability (in percentages).

Scanning electron microscopy (SEM) imaging was also used to visualize the biofilms and to confirm these results. Overall, the multispecies nature of the biofilms was validated by this procedure since cocci, rods and filaments, as well as spirochetes, were present within the biofilms, forming mixed communities (Fig. 2). The untreated samples revealed biofilms that had well organized network structures with virtually no dead or compromised bacterial cells (Fig. 3). However, cell lysis was evident after treatment for 10 minutes with CHX and CHX-Plus, and cell killing was even more pronounced at one week post-treatment (Fig. 3). The number of lysed or damaged cells substantially decreased five weeks after treatment and was practically nonexistent eight weeks after exposure to CHX-Plus (Fig. 3). The thickness of the biofilm decreased from 110 ± 15 μm before treatment to between 53.8 ± 1.8 and 66.0 ± 1.1 μm immediately after the different treatments. Contraction in the biofilms continued for one week after the treatments (between 32.8 ± 3.1 μm and 52.4 ± 6.5 μm) and stopped soon after it. The thickness of the biofilm eight weeks after the treatments did not return to its original size and was between 31.8 ± 2.9 μm and 42.2 ± 4.0 μm.

Numerical Results

Mathematical Model and its Calibration

In this model, a conversion mechanism between the susceptible and persister cells was assumed in addition to a regulatory role for quorum-sensing molecules in bacterial biofilm growth and EPS production. The model was calibrated against the data obtained for the biofilm treated with

CHX for 1, 3 and 10 minutes, respectively, at various stages of its natural growth in our previous [26] and current experiments. Specifically, we adjusted the model parameters to match the dead bacterial population with respect to the three treatments at several selected days when the experimental data were available. One set of the experimental data was plotted as Figure 1; additional experimental data and the model prediction were plotted in Figure 4 and Figure 5, respectively. The values of the model parameters during this calibration are summarized in Table 1 [27,28]. This set of model parameters was then used to predict the biofilm dynamics in the above-described study. The calibration of the model aimed to enable the selection of model parameters that would optimize the model prediction for the dead bacteria data as well as data for live bacteria from the samples cultured for three weeks before the CHX treatment until eight weeks after the treatment, as well as the dead bacterial population at a set of selected treatment days shown in Figure 4 (A). The coupled ordinary differential equations (ODEs) in the model were solved using a Matlab built-in function: ode45.

Antimicrobial Efficacy of Chlorhexidine against Bacteria in Biofilms at Different Stages of Development

Using the model, we investigated the persistence of biofilms of different ages in response to antimicrobial agents. In the experiments, biofilms were grown in the lab for up to a maximum of 12 weeks. We calculated the killing rate, which was defined as the dead bacterial volume fraction divided by the total bacterial volume fraction of the bacterial cells, by 1, 3 and 10 minute CHX treatments at various times, as well as for the control set at various ages of grown biofilms. The result is shown in Figure 4(A). These numerical simulations agreed well with the experimental results obtained in our previous study [26], which attested to the applicability of the mathematical model.

These analyses revealed that the killing proportion was, in general, a decay function of the biofilm age, i.e., the older the biofilm, the lower the killing proportion. However, three distinct and well-separated regimes for the killing proportion behavior existed with respect to age distribution. High killing proportions were observed for young biofilms, where the killing proportions reached as high as 78% in biofilms treated by CHX for 10 minutes. Even for the

biofilm treated by CHX for 1 minute, the killing proportions were as high as 63%. The killing proportions decayed slowly for the biofilms that were less than 10 days old. For biofilms between the age of 10 and 20 days, the killing proportions decayed much more drastically with age. The proportion of killed bacteria was much lower in biofilms 20 days or older than in young biofilms of 2-10 days. After 20 days, the proportion of killed bacteria remained low and relatively unchanged.

The simulation results was shown in Fig. 4B that the thickness of the biofilm was proportional to the bacterial volume fraction, consistent with experimental investigations in our previous study [26]. In addition to the results shown, the model was capable of providing more details about the composition of the biofilm. Both the biofilm thickness and the EPS volume fraction reached a plateau after about 24 days when the growth of the bacteria started slowing down; whereas the QS molecules kept increasing until their concentration eventually reached a plateau after about 50 days. Apparently, the increase in the concentration of the QS molecules had little impact on the growth of the bacterial population as this growth slowed down between the 25th and the 50th day.

Oral multispecies biofilm recovery after CHX treatment

Based on the model which simulated the susceptibility of biofilms at different phases of growth, we further investigated biofilm recovery after CHX treatment. In particular we chose as our initial example the three-week-old biofilm after treatment by CHX, without inactivator, for 1, 3 and 10 minutes. In the model, we assumed that the post-antibiotic effect was due to residual antimicrobial agents in the biofilm. The numerical results, together with experimental data are shown in Fig. 6A. Quantitatively, the mathematical model agreed well with the experimental data.

The longer the CHX treatment, the longer it took for the biofilm to regain its initial viability levels. The regrowth of the bacterial population correlated with the decrease and depletion of the antimicrobial agents in the biofilm (Fig. 5B). Both the susceptible and persistent cell populations

recovered at specific stages in this study, wherein the population of persistent cells changed because of the on-going conversion between the susceptible and persister cells (Fig. 5C).

Discussion

Endodontic infections can be defined as infections of the pulp and periapical tissues. There are several possible ways by which bacteria may enter the pulp, through caries lesions, enamel and dentin cracks, fractures, open dentin tubules, lateral canals, leaking fillings and rarely also via anachoresis. The multispecies biofilm model used in the present study does not completely replicate root canal biofilm. However, this model does capture some key characteristics of *in vivo* endodontic biofilms, including the thickness of the biofilm, multispecies nature, and the attachment of bacterial cells to each other. In particular, the collagen-coated hydroxyapatite provides chemical similarity with the teeth/dentin and serves as an excellent substrate for multispecies biofilm growth [26,29-31]. In the study reported here, this model was used to evaluate the effects of high levels of CHX on biofilms formed by bacterial samples isolated from the subgingival plaque of individual human subjects. We expected to observe extensive cell damage and consequent eradication of the biofilm as a result of the different treatments. Since the primary effect of CHX on bacteria is damage to the cell membrane [32,33], the effect of CHX can be readily visualized by vital staining [26,29,31,34,35]. Here we chose to use differential LIVE/DEAD staining rather than CFU counts to assess the ratio of live-to-dead cells over time, since this method has been shown to more accurately assess the true viability of cells within biofilms under adverse conditions (such as the presence of CHX) [30]. The results obtained during the first week post-treatment revealed the expected increase in dead biofilm cells (Fig. 1). However, after the first week of population decline, viable cells increased within the biofilm population and were eventually restored to a mature biofilm after eight weeks, independent of the treatment (Fig. 1). Confocal laser scanning microscopy imaging confirmed the overall trend observed in viability experiments. These data highlighted the inability of high concentrations of CHX to completely kill all cells in the biofilm, and suggested the presence of a subpopulation of biofilm cells (persisters) capable of tolerating such treatments, that eventually drove the eventual complete recovery of the biofilm.

To better understand the dynamics of the antimicrobial tolerance mechanisms, the mathematical modelling was used to extend information gained from *in vitro* experimentation in this study. There are several tolerance mechanisms together playing an important role in the failure of disinfection of biofilms. The persister population has been estimated to constitute perhaps 0.1–1% of all cells in a biofilm [36,37]. These cells, it is hypothesized, can survive a catastrophic antimicrobial challenge and reseed the biofilm. Biofilms are microbial communities encased by EPS. The EPS matrix provides several functional purposes for the biofilm, such as protecting bacteria from environmental stresses, and providing mechanical stability [38,39]. Quorum sensing is a density-dependent cell-cell communication mechanism used by several bacterial taxa to coordinate gene expression and behaviour in groups, based on population densities [40-42]. The advantage of mathematical models is they provide insights into the effect of various factors on the hypothetical mechanisms of antimicrobial biofilms. Such models can also minimize the number of experiments needed to investigate complex biological processes. Most previous models have simplified the analysis by focusing on a specific aspect (e.g. the bacterial population, formation of persisters, EPS production or QS regulation) in suspended bacteria cultures or on the initial stages of biofilm growth [43-49]. In the current study, our modeling incorporated each of those factors pertaining to the antimicrobial tolerance mechanisms including the bacterial volume fractions of susceptible, persister and dead cells, the EPS volume fraction, the concentration of the QS molecules, the nutrient concentration and the concentration of antimicrobial agents in oral biofilms at different physiological phases. Biofilms treated by both 2% CHX and CHX-Plus showed very similar susceptibility. Therefore, to explore the dynamics of the tolerance mechanisms, our mathematical model only simulated biofilms treated by 2% CHX and the subsequent recovery process.

Drug diffusion, especially of cationic antibiotics, is limited within biofilms due to the presence of an extensive negatively-charged EPS matrix, which hinders the diffusion of CHX into the deepest layers of the biofilms and thus its overall activity. A previous study [26] showed that the proportion of killed bacteria in mature biofilms was much lower than in young biofilms. This was consistent with our mathematical model, which simulated the dynamic process of oral multispecies biofilm at different ages after treatment with CHX (Fig. 4C). This model verified

that EPS prevents CHX from penetrating into the biofilm, thus making mature biofilm more difficult to treat compared with a young biofilm. In our model, we dealt with this effect as a kinetic issue rather than a spatial diffusive effect of antimicrobial agents. The mathematical model was proven to be an effective tool for analyzing the biofilm treatment with CHX. Recently, application of a different mathematical model correctly predicted that QS enabled bacteria to turn on and off the secretion of EPS, thus altering their ability to compete with other species and strains within mixed biofilm [42]. The effects of QS are highly variable and depend both upon the species under observation and the experimental conditions [48]. In the current study, when the thickness of mature biofilms (after 3-weeks old) reached a "steady state", EPS production also reached a plateau of accumulation. Conversely, QS molecule concentrations increased for up to 50 days before it reached a steady state. After three-weeks, therefore, QS molecules showed little influence on EPS production. The findings of the current study may help guide researchers to understand the interconnections between biofilm growth, QS and EPS production and how these impact on biofilm development and susceptibility to antimicrobial agents.

Previous studies have shown that treatment with 0.2% CHX significantly inhibits multispecies oral biofilms [34,50]. More specifically, exposure to 0.2% CHX induced biofilm cell killing and caused multispecies biofilms to contract at a rate of 1.176 $\mu m.min^{-1}$ over a period of 15 minutes. It was hypothesized that the mechanisms underlying the immediate contraction of oral biofilms upon exposure to CHX were related to ionic interactions between the negatively charged EPS matrix, which comprises the bulk of the volume of biofilms, and the positively charged CHX molecules. These interactions would change the solubility, hydrophobicity, and localized charge along the polymer chains of the EPS. Changes in charge would in turn affect the tertiary structure of the EPS chains and the degree of bonding with adjacent strands. As the positive CHX interacts with the negative EPS, the net charge of the matrix shifts toward neutral, reducing the repulsive forces between charged moieties, possibly allowing closer associations to occur between polymeric strands, may thus reduce the volume occupied by the biofilm. These concepts are consistent with the results obtained in the present study, which indicated that the thickness of biofilms decreased by around 50% after treatment with 2% CHX (from 110 μm before treatment

to 53-66 μm). Biofilm contraction continued for one week after the treatments, correlating with an increase in dead cells (Fig. 1).

It was previously shown that as little as 0.02% CHX kills biofilm cells [34,50]. In this study, we tested the susceptibility of multispecies oral biofilms to 10-times the concentration of CHX (2% CHX) used previously by Hope and Wilson [51], in an attempt to kill all of the cells present in our multispecies biofilms. Surprisingly, this concentration of CHX was insufficient to fully eradicate oral multispecies biofilms, thus indicating that additional antimicrobial compounds that synergize with CHX might be required to prevent biofilm re-growth in the root canal and in other contexts.

The ability of an antimicrobial to preserve its activity over time is an attractive property, as often the concentrations of antimicrobial agents tend to drop below the minimum inhibitory concentration thus no longer exerting the desired activity. Importantly, CHX has been shown to exhibit extended residual activity over time, a phenomenon called “substantivity” [52,53] or “post-antibiotic effect” [54]. The mathematical model predicted that post-antibiotic effect in the current study was due to residual antimicrobial agents in the biofilm. Indeed, an *in vivo* study on the mechanism of action of CHX [55] indicated that CHX inhibits plaque by an immediate bactericidal action followed by prolonged bacteriostatic activity of the CHX adsorbed onto the pellicle-coated enamel. Another report evaluating the substantively of 2% CHX within the bovine root canal system, after 10 minutes of application, reported that CHX retained antimicrobial activity even 12 weeks after the initial treatment [56]. Therefore, these previously published results imply that the oral multispecies biofilms presented in this report are quite resistant to high levels of CHX, as the activity of CHX is known to be preserved over long periods of time.

Accurate determination of antimicrobial effectiveness is another important property of an antimicrobial agent. This is measured by the ability of a particular compound to kill microorganisms in a specific amount of time. Hence, appropriate determination of antimicrobial activity requires complete and immediate inactivation (neutralization) of the antimicrobial agent. Ideally, all microorganisms used in evaluating antimicrobial effectiveness should be tested using

such an inactivation assay. The effectiveness of inactivation is strongly influenced by the concentration of the active agents, the amount of neutralizing agents, the storage time of the inactivated antiseptic before plating, and by the chosen microorganism. The combination of 3% Tween 80 and 0.3% L-α-lecithin has been found to be the most effective inactivating agent for CHX added to planktonic *E faecalis* and mixed plaque bacteria, allowing full recovery of the test organisms [57,58]. In the present study, the use of this inactivating agent had no effect on the activity of the different CHX formulations (Fig. 1), possibly due to its inability to penetrate into the biofilm over the time periods tested.

Our model indicated that the existence of persister cells, which are found in a small portion of the dominant bacteria persisting after to CHX antimicrobial treatment, was the main reason for relapse. Persisters would remain in a dormant state promoting tolerance to high concentrations of CHX. However, when the concentration of CHX would drop below the threshold at which it was no longer fatal to bacteria, the persisters would become metabolically active, converting into susceptible cells and beginning to multiply. Thus, the relative reduction of levels of persister cells in the present study was possibly due to the transformation between persister and susceptible cells. Further research is needed to isolate native persisters from the biofilm using cell sorting methods and investigate their transformation into rapidly growing susceptible cells. Nevertheless this conversion was indeed incorporated in the mathematical model developed.

In conclusion, this report describes the ability of oral multispecies biofilms to withstand complete killing by levels of CHX that substantially exceed those concentrations known to kill a proportion of cells within biofilms. This tolerance might be explained by the presence of persister cells within the biofilm population that led to biofilm recovery over time. Traditionally, the post-antibiotic effect of CHX suggested that the antimicrobial and antibiofilm activity of this compound would continue over long periods of time. Here we show that bacteria in biofilms eventually re-grow despite the presence of residual levels of CHX. Quantitatively, our mathematical model agrees well with the experimental phenomenon. The model provided results consistent with the hypothesis of the existence of persisters in biofilm. From a clinical perspective, these results have implications for determining the optimal interval between CHX

treatment of oral biofilms, and also define the inability of even the most active CHX formulations tested to completely kill oral biofilms. Also, the data presented here are consistent with the suggestion that recalcitrant oral biofilms may be responsible for difficult-to-treat root canal infections. In addition, our findings may relate to different types of oral biofilms and other biofilm-related fields of study. It appears necessary to identify compounds that synergize with CHX to prevent biofilm re-growth. The results presented here cannot be directly extrapolated to the root canal in human patients, but they serve as a guide for future investigations in the field of endodontic and oral biofilms. The simulation shows that mathematical modeling appears to be a useful tool for analyzing and predicting the effects of antimicrobial agents on bacterial biofilms, and further understanding the role that persister cells play in resistance to antimicrobials.

Materials and Methods

Experiment Development

Sterile hydroxyapatite (HA) discs (9.7 mm diameter by 1.5 mm thickness; Clarkson Chromatography Products, Williamsport, PA) were used as the biofilm substrate. The HA discs were coated with bovine dermal type I collagen (10 µg/mL collagen in 0.012 N HCl in water) (Cohesion, Palo Alto, CA) as previously described [26,29-31]. Subgingival plaque was collected and suspended in Brain Heart Infusion broth (BHI, Becton Dickinson, Sparks, MD, USA). This work was approved by the Clinical Research Ethics Board of the University of British Columbia, Canada (H12-00907), written informed consent was obtained [28]. The discs were incubated under anaerobic conditions (AnaeroGen, OXOID, Hampshire, UK) at 37˚C for 21 days; fresh medium was changed once a week. After 21 days of anaerobic incubation in BHI broth, specimens were then immersed in 2 mL of either 2% CHX freshly prepared from 20% stock solution (Sigma Chemical Co, St Louis, MO) or CHX-Plus (< 2% CHX gluconate solution with surface modifiers) (Vista Dental Products, Racine, WI) for 1, 3, or 10 minutes. The inactivator contained 1g α-Lecithin, 3 mL Tween 80, and 100 mL distilled water. After treatment, inactivator (2 mL) was applied for 60 s to inactivate chlorhexidine in half of the specimens. All specimens were then allowed to recover for the following eight weeks with the addition of fresh BHI broth once a week. Twelve specimens tested with saline for corresponding time periods were used as controls. For these specimens, the medium was changed once a week for eight weeks. Samples for CLSM

for viability staining were collected immediately and 1, 2, 3, 5, 7 and 8 weeks after the exposure to the medicaments. Samples for scanning electron microscopy (SEM) were collected immediately and 1, 3, 5 and 8 weeks after the treatments.

SEM Examination

Two biofilm specimens in each group were cut into four sections and measured for biofilm thickness by SEM (Helios Nanolab 650, FEI, Eindhoven) operating at 10 kV. The specimens were washed with phosphate-buffered saline for 5 minutes. Fixation was performed by adding 2.5% glutaraldehyde for 30 minutes and 1% osmium tetroxide (OsO_4) for 1 hour. The specimens were dehydrated by increasing concentrations of ethanol, dried by using a critical point drier (Samdri-795; Tousimis Research Corporation, Rockville, MD), and sputter-coated with gold-palladium in a vacuum evaporator (Hummer VI; Technics West Inc, Anaheim, CA). The thickness of three random areas of the biofilm on each piece was measured using ImageJ software (ImageJ 1.34n; National Institutes of Health, Bethesda, MD).

CLSM Analysis

The biofilm discs for CLSM imaging were rinsed in 0.85% physiological saline for 2 minutes to remove the culture broth. Two biofilm discs were examined for each time period. Five random areas of the biofilm on each disc were scanned (10 areas in each group; a total of 910 area scans for the whole study). To distinguish between live and dead cells, LIVE/DEAD *BacLight* Bacterial Viability kit L-7012 for microscopy and quantitative assays (Molecular Probes, Eugene, OR), which contained separate vials of the two component dyes (SYTO 9 and propidium iodide in 1:1 mixture) in solution, was used to stain the biofilm, following the manufacturer's instructions. The excitation/emission maxima for these dyes are 480/500 nm for the SYTO 9 stain and 490/635 nm for propidium iodide. Fluorescence from the stained cells was viewed using a CLSM (Nikon Eclipse C1, Nikon Canada, Mississauga, ON), equipped with Nikon Image analysis software. Simultaneous dual channel imaging was used to display green and red fluorescence.

CLSM images of the biofilms were acquired by the EZ-C1 v. 3.40 build 691 software (Nikon) at a resolution of 512 x 512 pixels. Individual biofilm images covered an area of 1.64 mm^2 per field of view. The mounted specimens were observed using a 10 x lens. Confocal LIVE/DEAD images were analyzed and quantitated using the Imaris 7.2 software (Bitplane Inc, St Paul, MN). The volume ratio of green fluorescence (live cells) to green-and-red fluorescence (live and dead cells) indicated the portion of live cells in the biofilm at each time. The method has been described in detail in previous studies [26,29-31]. The results were analyzed using Univariate ANOVA followed by post hoc analysis at a significance level of $P < 0.05$.

Mathematical Model Formulation

Model assumptions and derivation

A mathematical model was developed to describe the reactive kinetics in the biofilm system. The experimental data were obtained from our previous study (biofilms treated by CHX for 1, 3 and 10 minutes) [26] and current experiment (biofilms over time after exposure to CHX). In this model, the bacteria were modeled in three phenotypes: the susceptible (the ones that were susceptible to antimicrobial agents), the persister (the ones that were persistent to antimicrobial agents), and the dead bacteria. Their volume fractions were denoted, respectively, as S, P and D. Besides the bacteria, the volume fraction of the EPS and solvent were also calculated, which are denoted by E and T respectively. We assumed the material mixture constituting the biofilm was incompressible. By definition,

$$S + P + D + E + T = 1. \qquad (1)$$

Experiment evidence showed that bacteria would undergo a lag phase once transferred into new circumstances. To account for this physiological and regulatory lag process of biofilm formation, we introduced a phantom component named growth factor in this draft, to regulate cell proliferation. It represents the necessary signal molecules or proteins, or extra-cellular DNA produced in lag phase[59-61], which would affect cell proliferation (cell binary division), as well as the synchronization of quorum sensing molecules in a later stage.

For the functional components whose molecules were small compared with the components comprising the biomass; we disregarded their mass in the model. We classified the nutrient, QS molecules, and antimicrobial agents into this class of functional biofilm components. We denoted the concentration of nutrients, QS molecules, antimicrobial agents and functional molecules or growth factors as C, H, A and Q, respectively. Although their mass was neglected, their chemical and biological effects were prominent and thereby retained.

Reactive Equations for different Phenotypes of Bacteria

We assumed both susceptible bacteria and persister bacteria can proliferate following a logistic model with the growth rate regulated by the growth factor[62], antimicrobial agents[63] and nutrient. In has been proposed that the susceptible and the persister cells could convert to each other[64]. The rate of conversion from susceptible to persister cells was denoted as b_{sp} and the inverse conversion rate was denoted as b_{ps}. In addition, we denoted the natural death rate for the susceptible bacteria by r_{bs}. The antimicrobial agents killed susceptible and persister cells at different rates, which are denoted as c_3 and c_{12}, respectively. The killing rate for persisters was presumably very low[65] (which is the reason why they are named as persisters). Summarizing the mechanisms assumed above, we proposed the reactive equation for susceptible bacteria and persisters as follows

$$\frac{dS}{dt} = c_2 \frac{Q^2}{k_Q^2 + Q^2} \frac{k_{12}^2}{A^2 + k_{12}^2} \frac{C}{C + k_2} (1 - \frac{S}{S_{\max}}) S - b_{sp} S + b_{ps} P - r_{bs} S - \frac{c_3 \gamma A}{A + k_3} S, \quad (2)$$

$$\frac{dP}{dt} = c_4 \frac{Q^2}{k_Q^2 + Q^2} \frac{k_{12}^2}{A^2 + k_{12}^2} \frac{C}{C + k_2} (1 - \frac{P}{P_{\max}}) P + b_{sp} S - b_{ps} P - \frac{c_{12} \gamma A}{A + k_3} P, \quad (3)$$

where $S_{\max}$ is the carrying capacity for the susceptible bacteria and k_{12}, k_3 are the half salutation rate for hill type reactive kinetics. Here γ is the slow-penetration factor, which is proposed in the Hinson model as follows[66]

$$\gamma = \frac{1}{T + \frac{E}{D_{pr}}} \frac{2(T + E)}{2 + (S + P + D)}. \quad (4)$$

The prefactors in the form of Hill-type functions are postulated and calibrated to achieve the best fitting result.

The concentration of the dead bacteria was governed by the following reaction equation:

$$\frac{dD}{dt} = \left(r_{bs} + c_3 \frac{\gamma A}{A + k_3} \right) S + c_{12} \frac{\gamma A}{A + k_3} P - r_{dp} \frac{k_{13}}{k_{13} + A} \frac{D}{D + k_{15}} D, \tag{5}$$

where, on the right hand side, the first two terms were the growth terms due to the death of susceptible and persister cells, respectively, and the last term represents the break down of dead bacteria into EPS and solvent components due to cell lysis[67]. Here r_{dp} is the maximum break down rate of dead bacteria, and k_{13}, k_{15} are the half salutation rate.

Reactive Equation for EPS production

For EPS production, we considered that live bacteria produce EPS with a growth rate affected by the concentration of nutrient and quorum-sensing molecules[68-70]. The mechanism was effectively modeled by the Hill type kinetic equation. Since quorum sensing molecules affect the gene expression of the bacterial cells, they regulate effectively the EPS production by both susceptible and persister cells. Besides, we required that the rate of EPS production be reduced as the concentration of EPS increased. The dead bacteria can disintegrate to shed their surface-attached EPS[67], which contributed to the second term in the following reactive equation. The reactive equation was thus proposed as follows:

$$\frac{dE}{dt} = c_5 (S + P) \frac{C}{C + k_2} \frac{H^2}{H^2 + k_9^2} (1 - \frac{E}{E_{\max}}) + r_{dp} \frac{k_{13}}{k_{13} + A} \frac{D}{D + k_{15}} D, \tag{6}$$

where the first part was the gain of EPS due to the live bacteria and the second part was that gain from the dead bacterial conversion. Here c_5 is the maximum production EPS production rate due to live bacteria and k_2, k_9 are the half salutation rates.

Reactive Equations for Functional Components

For nutrient and antimicrobial agent concentration, the monod model was appropriate. For the QS molecules and growth factors, however, their production depended on the concentration of the susceptible bacteria while, in the meantime, saturate at a maximum level in the presence of a large number of the QS molecules or growth factors. For these molecules, we thus proposed a coupled system of reactive equations:

$$\frac{dC}{dt} = -c_7(S+P)\frac{C}{C+k_2}, \tag{7}$$

$$\frac{dA}{dt} = -c_8(S+P)\frac{A}{k_8+A} - r_a A, \tag{8}$$

$$\frac{dH}{dt} = c_A S\frac{Q^2}{k_Q^2+Q^2}(1-\frac{H}{H_{\max}}), \tag{9}$$

$$\frac{dQ}{dt} = c_q S(1-\frac{Q}{Q_{\max}}), \tag{10}$$

where c_7, c_8 are the maximum consumption rates for nutrient and antimicrobial agents, correspondingly. And c_A, c_q are the maximum production rate for QS molecules and growth factors, respectively. k_2, k_8 are the half salutation rates, and r_a is the natural decay rate, indicating that the antimicrobial agents would lose its effects in time. Here $H_{\max}$, $Q_{\max}$ are the saturation level for QS molecules and growth factors.

Summary of the Governing Equations

In summary, the coupled ordinary differential equations for biofilm model were given as follows

$$
\begin{aligned}
\frac{dS}{dt} &= c_2 \frac{Q^2}{k_2^2+Q^2} \frac{k_{12}^2}{A^2+k_{12}^2} \frac{C}{C+k_2}(1-\frac{S}{S_{\max}})S - b_{sp}S + b_{ps}P - r_{bs}S - \frac{c_3\gamma A}{A+k_3}S, \\
\frac{dP}{dt} &= c_4 \frac{Q^2}{k_Q^2+Q^2} \frac{k_{12}^2}{A^2+k_{12}^2} \frac{C}{C+k_2}(1-\frac{P}{P_{\max}})P + b_{sp}S - b_{ps}P - \frac{c_{12}\gamma A}{A+k_3}P, \\
\frac{dD}{dt} &= \left(r_{bs} + c_3\frac{\gamma A}{A+k_3}\right)S + c_{12}\frac{\gamma A}{A+k_3}P - r_{dp}\frac{k_{13}}{k_{13}+A}\frac{D}{D+k_{15}}D, \\
\frac{dE}{dt} &= c_5(S+P)\frac{C}{C+k_2}\frac{H^2}{H^2+k_9^2}(1-\frac{E}{E_{\max}}) + r_{dp}\frac{k_{13}}{k_{13}+A}\frac{D}{D+k_{15}}D, \\
\frac{dC}{dt} &= -c_7(S+P)\frac{C}{C+k_2}, \\
\frac{dA}{dt} &= -c_8(S+P)\frac{A}{k_8+A} - r_a A, \\
\frac{dH}{dt} &= c_A\frac{Q^2}{Q^2+k_Q^2}S(1-\frac{H}{H_{\max}}), \\
\frac{dQ}{dt} &= c_q S(1-\frac{Q}{Q_{\max}}),
\end{aligned}
$$

Where

$$
\gamma = \frac{1}{T+\frac{E}{D_{pr}}}\frac{2(T+E)}{2+(S+P+D)}. \qquad (11)
$$

Here we use c_0 d_0 $H_{\max}$ and $Q_{\max}$, as well as t_0 to non-dimensionalize the system. Thus, in later discussion, the concentration of non-dimensionalized functional molecules range from 0 and 1 in later context. To obtain the solution of these equations, we used an ODE solver in Matlab. The model parameters were first calibrated against the experiments alluded to in the previous sections. This model can be readily extended to include spatial convection and diffusion to describe any heterogeneous effects in biofilm colonies.

References

1 Picioreanu, C., van Loosdrecht, M. C. M. & Heijnen, J. J. Mathematical modeling of biofilm structure with a hybrid differential-discrete cellular automaton approach. *Biotechnol Bioeng* **58**, 101-116, doi:Doi 10.1002/(Sici)1097-0290(19980405)58:1<101::Aid-Bit11>3.0.Co;2-M (1998).

2 Kakehashi, S., Stanley, H. R. & Fitzgerald, R. J. The effects of surgical exposures of dental pulps in germfree and conventional laboratory rats. *J South Calif Dent Assoc* **34**, 449-451 (1966).

3 Peter, H. *et al.* Multifunctionality and diversity in bacterial biofilms. *PLoS One* **6**, e23225, doi:10.1371/journal.pone.0023225 PONE-D-11-04601 [pii] (2011).

4 Peters, L. B., Wesselink, P. R., Buijs, J. F. & van Winkelhoff, A. J. Viable bacteria in root dentinal tubules of teeth with apical periodontitis. *J Endod* **27**, 76-81, doi:S0099-2399(05)60701-7 [pii] 10.1097/00004770-200102000-00002 (2001).

5 Mah, T. F. & O'Toole, G. A. Mechanisms of biofilm resistance to antimicrobial agents. *Trends Microbiol* **9**, 34-39, doi:S0966-842X(00)01913-2 [pii] (2001).

6 Stewart, P. S. Diffusion in biofilms. *J Bacteriol* **185**, 1485-1491 (2003).

7 Zijnge, V. *et al.* Oral biofilm architecture on natural teeth. *PLoS One* **5**, e9321, doi:10.1371/journal.pone.0009321 (2010).

8 Folkesson, A., Haagensen, J. A., Zampaloni, C., Sternberg, C. & Molin, S. Biofilm induced tolerance towards antimicrobial peptides. *PLoS One* **3**, e1891, doi:10.1371/journal.pone.0001891 (2008).

9 Sjogren, U., Happonen, R. P., Kahnberg, K. E. & Sundqvist, G. Survival of Arachnia propionica in periapical tissue. *Int Endod J* **21**, 277-282 (1988).

10 Nair, P. N., Sjogren, U., Krey, G., Kahnberg, K. E. & Sundqvist, G. Intraradicular bacteria and fungi in root-filled, asymptomatic human teeth with therapy-resistant periapical lesions: a long-term light and electron microscopic follow-up study. *J Endod* **16**, 580-588, doi:S0099-2399(07)80201-9 [pii] 10.1016/S0099-2399(07)80201-9 (1990).

11 Figdor, D., Sjogren, U., Sorlin, S., Sundqvist, G. & Nair, P. N. Pathogenicity of Actinomyces israelii and Arachnia propionica: experimental infection in guinea pigs and phagocytosis and intracellular killing by human polymorphonuclear leukocytes in vitro. *Oral Microbiol Immunol* **7**, 129-136 (1992).

12 Ricucci, D., Siqueira, J. F., Jr., Bate, A. L. & Pitt Ford, T. R. Histologic investigation of root canal-treated teeth with apical periodontitis: a retrospective study from twenty-four patients. *J Endod* **35**, 493-502, doi:10.1016/j.joen.2008.12.014 S0099-2399(09)00004-1 [pii] (2009).

13 Sundqvist, G. Bacteriological studies of necrotic dental pulps. *Umae Univ Odontological Dissertations* **7**, 1-93 (1976).

14 Haapasalo, M., Shen, Y. & Ricucci, D. Reasons for persistent and emerging post-treatment endodontic disease. *Endod Topics* **18**, 31-50 (2008).

15 Ricucci, D. & Siqueira, J. F., Jr. Fate of the tissue in lateral canals and apical ramifications in response to pathologic conditions and treatment procedures. *J Endod* **36**, 1-15, doi:10.1016/j.joen.2009.09.038 S0099-2399(09)00825-5 [pii] (2010).

16 Ricucci, D. & Siqueira, J. F., Jr. Biofilms and apical periodontitis: study of prevalence and association with clinical and histopathologic findings. *J Endod* **36**, 1277-1288, doi:10.1016/j.joen.2010.04.007 S0099-2399(10)00379-1 [pii] (2010).
17 Haapasalo, M., Shen, Y., Qian, W. & Gao, Y. Irrigation in endodontics. *Dent Clin North Am* **54**, 291-312, doi:10.1016/j.cden.2009.12.001 S0011-8532(09)00109-8 [pii] (2010).
18 Waltimo, T. M., Orstavik, D., Siren, E. K. & Haapasalo, M. P. In vitro susceptibility of Candida albicans to four disinfectants and their combinations. *Int Endod J* **32**, 421-429 (1999).
19 Gomes, B. P. *et al.* In vitro antimicrobial activity of several concentrations of sodium hypochlorite and chlorhexidine gluconate in the elimination of Enterococcus faecalis. *Int Endod J* **34**, 424-428 (2001).
20 Radcliffe, C. E. *et al.* Antimicrobial activity of varying concentrations of sodium hypochlorite on the endodontic microorganisms Actinomyces israelii, A. naeslundii, Candida albicans and Enterococcus faecalis. *Int Endod J* **37**, 438-446, doi:10.1111/j.1365-2591.2004.00752.x IEJ752 [pii] (2004).
21 McDonnell, G. & Russell, A. D. Antiseptics and disinfectants: activity, action, and resistance. *Clin Microbiol Rev* **12**, 147-179 (1999).
22 Schlafer, S. *et al.* Osteopontin reduces biofilm formation in a multi-species model of dental biofilm. *PLoS One* **7**, e41534, doi:10.1371/journal.pone.0041534 PONE-D-12-12722 [pii] (2012).
23 Klapper, I. & Dockery, J. Mathematical description of microbial biofilms. *SIAM Rev* **52**, 221-265 (2010).
24 Wang, Q. & Zhang, T. Review of mathematical models for biofilms. *Solid State Commun* **150**, 1009-1022 (2010).
25 Lardon, L. A. *et al.* iDynoMiCS: next-generation individual-based modelling of biofilms. *Environ Microbiol* **13**, 2416-2434, doi:10.1111/j.1462-2920.2011.02414.x (2011).
26 Shen, Y., Stojicic, S. & Haapasalo, M. Antimicrobial efficacy of chlorhexidine against bacteria in biofilms at different stages of development. *J Endod* **37**, 657-661, doi:10.1016/j.joen.2011.02.007 S0099-2399(11)00112-9 [pii] (2011).
27 Keren, I., Kaldalu, N., Spoering, A., Wang, Y. & Lewis, K. Persister cells and tolerance to antimicrobials. *FEMS Microbiol Lett* **230**, 13-18, doi:S0378109703008565 [pii] (2004).
28 Zhang, T., Cogan, N. & Wang, Q. Phase field models for biofilms. I. Theory and one-dimensional simulations. *SIAM J. Appl. Math* **69**, 641-669 (2008).
29 Shen, Y., Qian, W., Chung, C., Olsen, I. & Haapasalo, M. Evaluation of the effect of two chlorhexidine preparations on biofilm bacteria in vitro: a three-dimensional quantitative analysis. *J Endod* **35**, 981-985, doi:10.1016/j.joen.2009.04.030 S0099-2399(09)00374-4 [pii] (2009).
30 Shen, Y., Stojicic, S. & Haapasalo, M. Bacterial viability in starved and revitalized biofilms: comparison of viability staining and direct culture. *J Endod* **36**, 1820-1823, doi:10.1016/j.joen.2010.08.029 S0099-2399(10)00687-4 [pii] (2010).
31 Shen, Y., Stojicic, S., Qian, W., Olsen, I. & Haapasalo, M. The synergistic antimicrobial effect by mechanical agitation and two chlorhexidine preparations on biofilm bacteria. *J Endod* **36**, 100-104, doi:10.1016/j.joen.2009.09.018 S0099-2399(09)00778-X [pii] (2010).

32 Brecx, M. & Theilade, J. Effect of chlorhexidine rinses on the morphology of early dental plaque formed on plastic film. *J Clin Periodontol* **11**, 553-564 (1984).
33 Vitkov, L. *et al.* Chlorhexidine-induced ultrastructural alterations in oral biofilm. *Microsc Res Tech* **68**, 85-89, doi:10.1002/jemt.20238 (2005).
34 Hope, C. K. & Wilson, M. Analysis of the effects of chlorhexidine on oral biofilm vitality and structure based on viability profiling and an indicator of membrane integrity. *Antimicrob Agents Chemother* **48**, 1461-1468 (2004).
35 Chavez de Paz, L. E. Image analysis software based on color segmentation for characterization of viability and physiological activity of biofilms. *Appl Environ Microbiol* **75**, 1734-1739, doi:10.1128/AEM.02000-08 AEM.02000-08 [pii] (2009).
36 Lewis, K. Persister cells, dormancy and infectious disease. *Nat Rev Microbiol* **5**, 48-56, doi:nrmicro1557 [pii] 10.1038/nrmicro1557 (2007).
37 Lewis, K. Persister cells. *Annu Rev Microbiol* **64**, 357-372, doi:10.1146/annurev.micro.112408.134306 (2010).
38 Davey, M. E. & O'Toole G, A. Microbial biofilms: from ecology to molecular genetics. *Microbiol Mol Biol Rev* **64**, 847-867 (2000).
39 Hall-Stoodley, L., Costerton, J. W. & Stoodley, P. Bacterial biofilms: from the natural environment to infectious diseases. *Nat Rev Microbiol* **2**, 95-108, doi:10.1038/nrmicro821 (2004).
40 Singh, P. K. *et al.* Quorum-sensing signals indicate that cystic fibrosis lungs are infected with bacterial biofilms. *Nature* **407**, 762-764, doi:10.1038/35037627 (2000).
41 Davies, D. G. *et al.* The involvement of cell-to-cell signals in the development of a bacterial biofilm. *Science* **280**, 295-298 (1998).
42 Hammer, B. K. & Bassler, B. L. Quorum sensing controls biofilm formation in Vibrio cholerae. *Mol Microbiol* **50**, 101-104, doi:3688 [pii] (2003).
43 Szomolay, B., Klapper, I., Dockery, J. & Stewart, P. S. Adaptive responses to antimicrobial agents in biofilms. *Environ Microbiol* **7**, 1186-1191, doi:EMI797 [pii] 10.1111/j.1462-2920.2005.00797.x (2005).
44 Roberts, M. E. & Stewart, P. S. Modelling protection from antimicrobial agents in biofilms through the formation of persister cells. *Microbiology* **151**, 75-80, doi:151/1/75 [pii] 10.1099/mic.0.27385-0 (2005).
45 Goryachev, A. B., Toh, D. J. & Lee, T. Systems analysis of a quorum sensing network: design constraints imposed by the functional requirements, network topology and kinetic constants. *Biosystems* **83**, 178-187, doi:S0303-2647(05)00126-7 [pii] 10.1016/j.biosystems.2005.04.006 (2006).
46 Cogan, N. G. Effects of persister formation on bacterial response to dosing. *J Theor Biol* **238**, 694-703, doi:S0022-5193(05)00275-4 [pii] 10.1016/j.jtbi.2005.06.017 (2006).
47 Xavier, J. B. & Foster, K. R. Cooperation and conflict in microbial biofilms. *Proc Natl Acad Sci U S A* **104**, 876-881, doi:0607651104 [pii] 10.1073/pnas.0607651104 (2007).
48 Nadell, C. D., Xavier, J. B., Levin, S. A. & Foster, K. R. The evolution of quorum sensing in bacterial biofilms. *PLoS Biol* **6**, e14, doi:10.1371/journal.pbio.0060014 07-PLBI-RA-3220 [pii] (2008).
49 De Leenheer, P. & Cogan, N. G. Failure of antibiotic treatment in microbial populations. *J Math Biol* **59**, 563-579, doi:10.1007/s00285-008-0243-6 (2009).

50 von Ohle, C. *et al.* Real-time microsensor measurement of local metabolic activities in ex vivo dental biofilms exposed to sucrose and treated with chlorhexidine. *Appl Environ Microbiol* **76**, 2326-2334, doi:10.1128/AEM.02090-09 AEM.02090-09 [pii] (2010).
51 Lewis, K. Persister Cells. *Annu Rev Microbiol* **64**, 357-372, doi:10.1146/annurev.micro.112408.134306 (2010).
52 Jeansonne, M. J. & White, R. R. A comparison of 2.0% chlorhexidine gluconate and 5.25% sodium hypochlorite as antimicrobial endodontic irrigants. *J Endod* **20**, 276-278 (1994).
53 White, R. R., Hays, G. L. & Janer, L. R. Residual antimicrobial activity after canal irrigation with chlorhexidine. *J Endod* **23**, 229-231, doi:S0099-2399(97)80052-0 [pii] 10.1016/S0099-2399(97)80052-0 (1997).
54 MacKenzie, F. M. & Gould, I. M. The post-antibiotic effect. *J Antimicrob Chemother* **32**, 519-537 (1993).
55 Jenkins, S., Addy, M. & Wade, W. The mechanism of action of chlorhexidine. A study of plaque growth on enamel inserts in vivo. *J Clin Periodontol* **15**, 415-424 (1988).
56 Rosenthal, S., Spangberg, L. & Safavi, K. Chlorhexidine substantivity in root canal dentin. *Oral Surg Oral Med Oral Pathol Oral Radiol Endod* **98**, 488-492, doi:S1079210403004815 [pii] 10.1016/S1079210403004815 (2004).
57 Zamany, A. & Spangberg, L. S. An effective method of inactivating chlorhexidine. *Oral Surg Oral Med Oral Pathol Oral Radiol Endod* **93**, 617-620, doi:S1079210402000197 [pii] (2002).
58 Stojicic, S., Shen, Y., Qian, W., Johnson, B. & Haapasalo, M. Antibacterial and smear layer removal ability of a novel irrigant, QMiX. *Int Endod J* **45**, 363-371, doi:10.1111/j.1365-2591.2011.01985.x (2012).
59 Brejning, J. & Jespersen, L. Protein expression during lag phase and growth initiation in Saccharomyces cerevisiae. *Int J Food Microbiol* **75**, 27-38, doi:Pii S0168-1605(01)00726-7 Doi 10.1016/S0168-1605(01)00726-7 (2002).
60 Gefen, O., Fridman, O., Ronin, I. & Balaban, N. Q. Direct observation of single stationary-phase bacteria reveals a surprisingly long period of constant protein production activity. *P Natl Acad Sci USA* **111**, 556-561, doi:10.1073/pnas.1314114111 (2014).
61 Larsen, N., Boye, M., Siegumfeldt, H. & Jakobsen, M. Differential expression of proteins and genes in the lag phase of Lactococcus lactis subsp lactis grown in synthetic medium and reconstituted skim milk. *Appl Environ Microb* **72**, 1173-1179, doi:10.1128/Aem.72.2.1173-1179.2006 (2006).
62 Baty, F. & Delignette-Muller, M. L. Estimating the bacterial lag time: which model, which precision? *Int J Food Microbiol* **91**, 261-277, doi:10.1016/j.ijfoodmicro.2003.07.002 (2004).
63 Brown, M. R. W., Collier, P. J. & Gilbert, P. Influence of Growth-Rate on Susceptibility to Antimicrobial Agents - Modification of the Cell-Envelope and Batch and Continuous Culture Studies. *Antimicrob Agents Ch* **34**, 1623-1628 (1990).
64 Balaban, N. Q., Merrin, J., Chait, R., Kowalik, L. & Leibler, S. Bacterial persistence as a phenotypic switch. *Science* **305**, 1622-1625, doi:10.1126/science.1099390 (2004).
65 Keren, I., Kaldalu, N., Spoering, A., Wang, Y. P. & Lewis, K. Persister cells and tolerance to antimicrobials (vol 230, pg 12, 2003). *Fems Microbiol Lett* **234**, 187-187, doi:10.1016/j.femsle.2004.03.006 (2004).

66 Hinson, R. K. & Kocher, W. M. Model for effective diffusivities in aerobic biofilms. *J Environ Eng-Asce* **122**, 1023-1030, doi:Doi 10.1061/(Asce)0733-9372(1996)122:11(1023) (1996).
67 Bayles, K. W. The biological role of death and lysis in biofilm development. *Nat Rev Microbiol* **5**, 721-726, doi:10.1038/nrmicro1743 (2007).
68 Marketon, M. M., Glenn, S. A., Eberhard, A. & Gonzalez, J. E. Quorum sensing controls exopolysaccharide production in Sinorhizobium meliloti. *J Bacteriol* **185**, 325-331, doi:10.1128/Jb.185.1.325-331.2003 (2003).
69 Vuong, C., Gerke, C., Somerville, G. A., Fischer, E. R. & Otto, M. Quorum-sensing control of biofilm factors in Staphylococcus epidermidis. *J Infect Dis* **188**, 706-718, doi:Doi 10.1086/377239 (2003).
70 Waters, C. M. & Bassler, B. L. Quorum sensing: Cell-to-cell communication in bacteria. *Annu Rev Cell Dev Bi* **21**, 319-346, doi:10.1146/annurev.cellbio.21.012704.131001 (2005).
71 Zhang, T. Y., Cogan, N. G. & Wang, Q. Phase Field Models for Biofilms. I. Theory and One-Dimensional Simulations. *Siam J Appl Math* **69**, 641-669, doi:10.1137/070691966 (2008).
72 Shen, Y., Qian, W., Chung, C., Olsen, I. & Haapasalo, M. Evaluation of the Effect of two Chlorhexidine Preparations on biofilm bacteria *in vitro*: A Three-Dimensional Quantitative Analysis. *J Endodont* **35**, 981-985, doi:10.1016/j.joen.2009.04.030 (2009).
73 Shen, Y., Stojicic, S. & Haapasalo, M. Antimicrobial efficacy of chlorhexidine against bacteria in biofilms at different stages of development. *J Endodont* **37**, 657-661, doi:10.1016/j.joen.2011.02.007 (2011).
74 Cogan, N. G. Effects of persister formation on bacterial response to dosing. *J Theor Biol* **238**, 694-703, doi:10.1016/j.jtbi.2005.06.017 (2006).
75 Lindley, B., Wang, Q. & Zhang, T. Y. A Multicomponent Model for Biofilm-Drug Interaction. *Discrete Cont Dyn-B* **15**, 417-456, doi:10.3934/dcdsb.2011.15.417 (2011).
76 Alpkvist, E. & Klapper, I. A multidimensional multispecies continuum model for heterogeneous biofilm development (vol 69, pg 765, 2007). *B Math Biol* **69**, 2445-2445, doi:10.1007/s11538-007-9212-2 (2007).
77 Alpkvist, E., Picioreanu, C., van Loosdrecht, M. C. M. & Heyden, A. Three-dimensional biofilm model with individual cells and continuum EPS matrix. *Biotechnol Bioeng* **94**, 961-979, doi:10.1002/bit.20917 (2006).

Figure legends

Figure 1. Proportion of live cells in a multispecies biofilm over time. A 3-week-old biofilm was treated either for 1, 3 or 10 minutes with the compounds indicated in the graph. The y-axis ratio corresponds to [live bacteria/(total bacteria)], given that green and red fluorescence indicate live and dead cells, respectively. Two microliters of inactivator were added for 60 seconds immediately after the different treatments. (— • — No Treatment, ■ CHX 1 minute with inactivator, □ CHX 1 minute without inactivator, ▲ CHX 3min with inactivator, △ CHX 3 minutes without inactivator, ● CHX 10min with inactivator, ○ CHX 10min without inactivator; ■ CHX-Plus 1 minute with inactivator, □ CHX-Plus 1 minute without inactivator, ▲ CHX-Plus 3 minutes with inactivator, △ CHX-Plus 3 minutes without inactivator, ● CHX-Plus 10 minutes with inactivator, ○ CHX-Plus 10 minutes without inactivator).

Figure 2. Scanning electron micrograph of biofilms with mixed bacterial flora including numerous spirochetes. Three-week old biofilm after being treated with 2% CHX for 3 minutes (A); (B-D) higher magnification of (A) showed tightly coiled spirochetes and a few damaged bacterial cells.

Figure 3. Scanning electron micrographs of biofilms untreated and treated with CHX-Plus over time.

Figure 4. Model prediction for the proportion of the dead cell volumes of biofilms treated by CHX, and the thickness of a naturally growing biofilm. The initial profile for each components are (0.056, 0.024, 0, 0, 1.0, 0, 0) for the volume fractions of suscep- tible, persister, dead bacteria and EPS, as well as the concentrations for nutrient, antimicrobial agents and QS molecules, respectively. (A) Percentage of dead bacterial cells in biofilms at different time of biofilm growth after being treated with CHX for 1, 3 and 10 minutes, respectively. The bottom line is the natural death as a controlled experiment (experimental data are obtained from[72]); (B) Biofilm thickness of controlled group.

Figure 5. Bacteria in biofilms after treated with CHX up to 8 weeks. The initial profile for bacteria components, EPS and QS molecules are from the simulation in figure 1 at 3 weeks. For the leftover concentrations of antimicrobial agents, they are fitted as 1.67×10^{-4}, 2.1×10^{-4} and 3.75×10^{-4} for CHX 1, 3, 10 minutes treatment correspondingly. The concentrations of nutrient are supported as 1. The percentage of live cell volume in biofilms during recovery after treatment with CHX for 1, 3, 10 minutes and the control set (without treatment), respectively. The longer the biofilm is treated with CHX, the longer it takes for the bacterial cells to regain their populations (experimental data are obtained from[71] and Fig. 1).

Figure 1. Proportion of live cells in a multispecies biofilm over time. A 3-week-old biofilm was treated either for 1, 3 or 10 minutes with the compounds indicated in the graph. The y-axis ratio corresponds to [live bacteria/(total bacteria)], given that green and red fluorescence indicate live and dead cells, respectively. Two microliters of inactivator were added for 60 seconds immediately after the different treatments. (— • — No Treatment, ■ CHX 1 minute with inactivator, □ CHX 1 minute without inactivator, ▲ CHX 3min with inactivator, △ CHX 3 minutes without inactivator, ● CHX 10min with inactivator, ○ CHX 10min without inactivator; ■ CHX-Plus 1 minute with inactivator, □ CHX-Plus 1 minute without inactivator, ▲ CHX-Plus 3 minutes with inactivator, △ CHX-Plus 3 minutes without inactivator, ● CHX-Plus 10 minutes with inactivator, ○ CHX-Plus 10 minutes without inactivator).

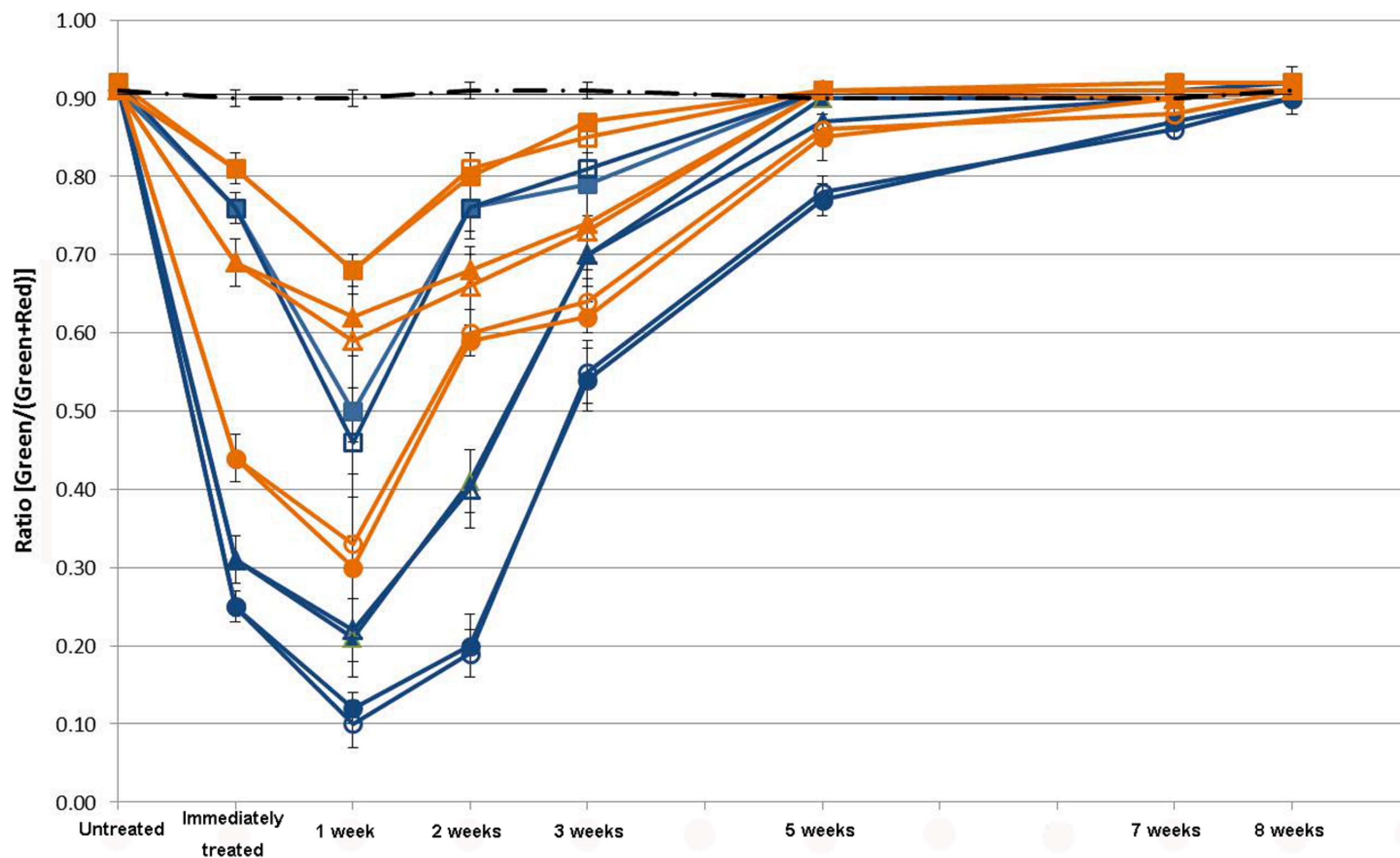

Figure 2. Scanning electron micrograph of biofilms with mixed bacterial flora including numerous spirochetes. Three-week old biofilm after being treated with 2% CHX for 3 minutes (A); (B-D) higher magnification of (A) showed tightly coiled spirochetes and a few damaged bacterial cells.

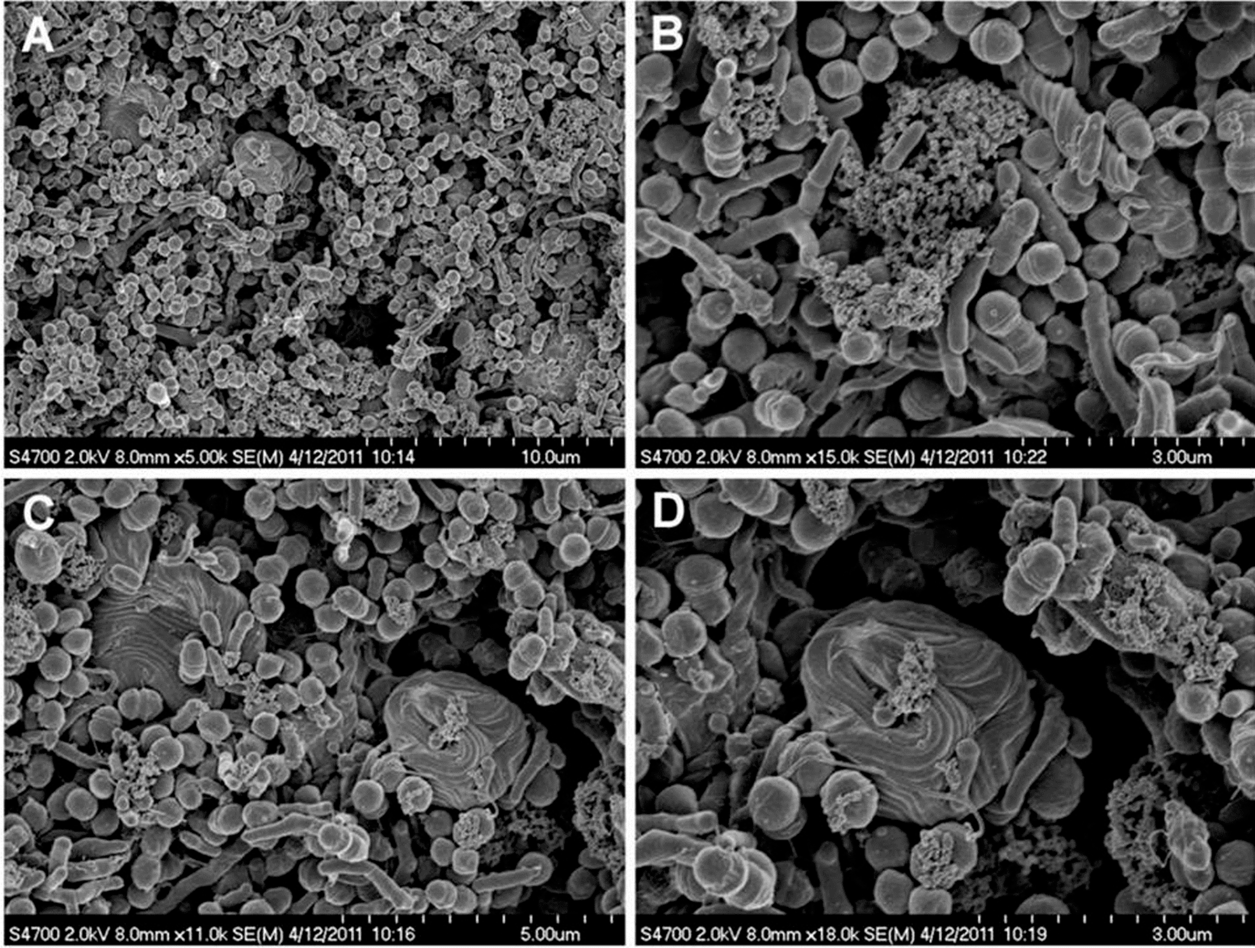

Figure 3. Scanning electron micrographs of biofilms untreated and treated with CHX-Plus over time.

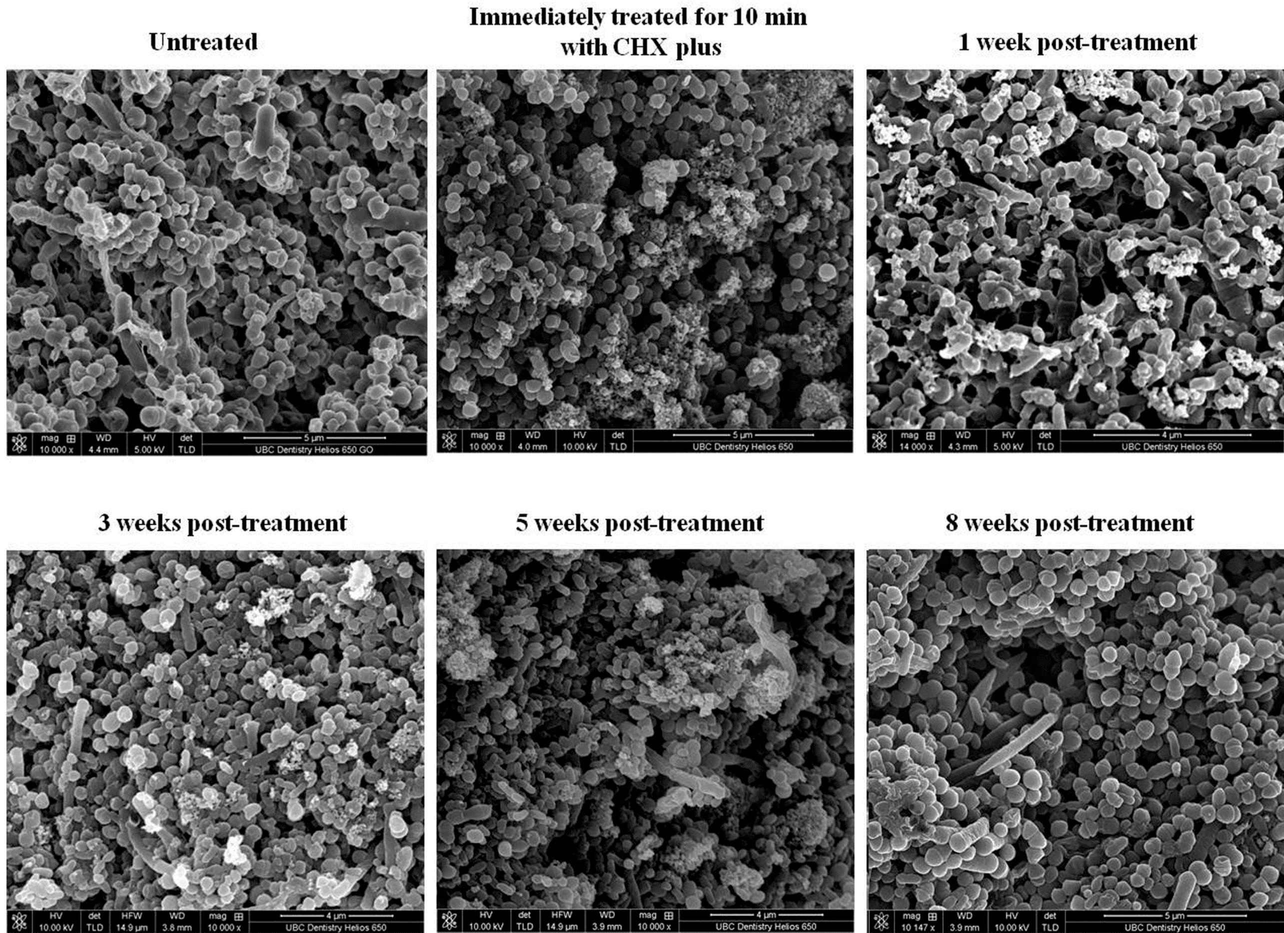

Figure 4. Model prediction for the proportion of the dead cell volumes of biofilms treated by CHX, and the thickness of a naturally growing biofilm. The initial profile for each components are (0.056, 0.024, 0, 0, 1.0, 0, 0) for the volume fractions of suscep- tible, persister, dead bacteria and EPS, as well as the concentrations for nutrient, antimicrobial agents and QS molecules, respectively. (A) Percentage of dead bacterial cells in biofilms at different time of biofilm growth after being treated with CHX for 1, 3 and 10 minutes, respectively. The bottom line is the natural death as a controlled experiment (experimental data are obtained from[72]); (B) Biofilm thickness of controlled group.

(A)

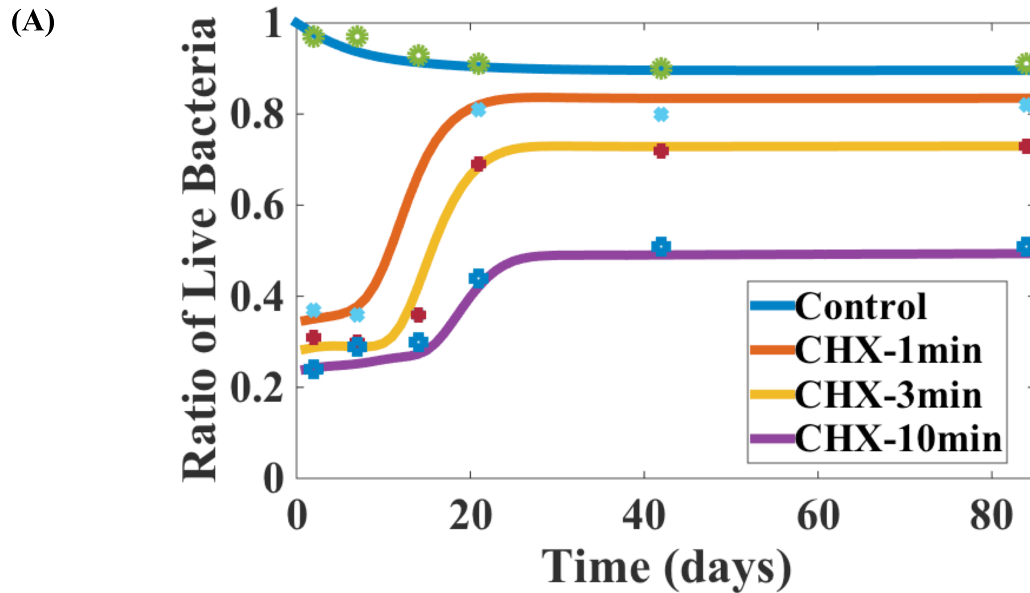

(B)

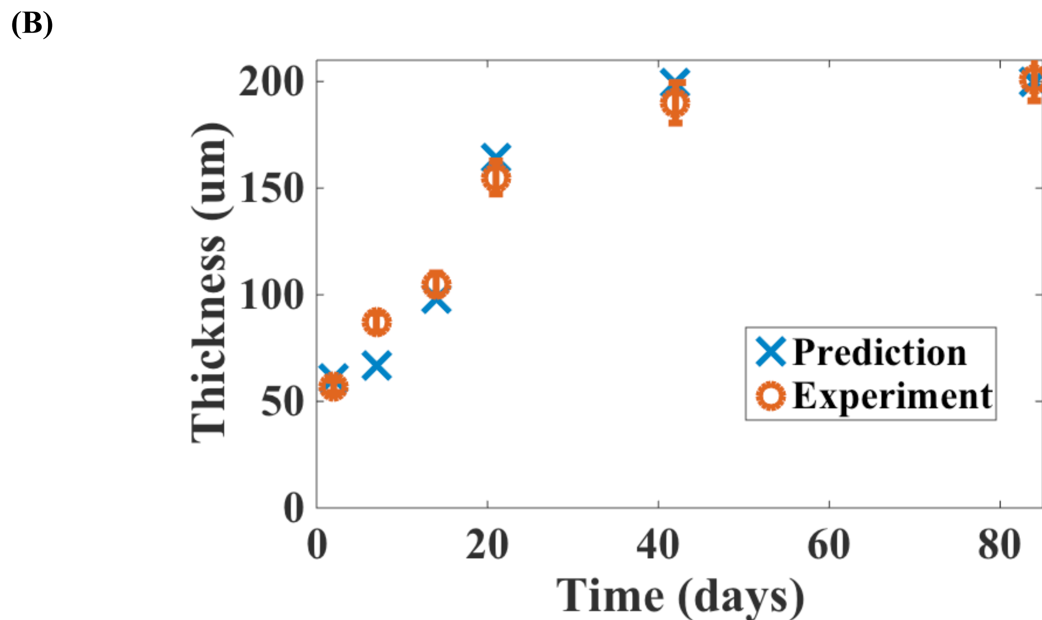

Figure 5. Bacteria in biofilms after treated with CHX up to 8 weeks. The initial profile for bacteria components, EPS and QS molecules are from the simulation in figure 1 at 3 weeks. For the leftover concentrations of antimicrobial agents, they are fitted as 1.67×10^{-4}, 2.1×10^{-4} and 3.75×10^{-4} for CHX 1, 3, 10 minutes treatment correspondingly. The concentrations of nutrient are supported as 1. The percentage of live cell volume in biofilms during recovery after treatment with CHX for 1, 3, 10 minutes and the control set (without treatment), respectively. The longer the biofilm is treated with CHX, the longer it takes for the bacterial cells to regain their populations (experimental data are obtained from[71] and Fig. 1).

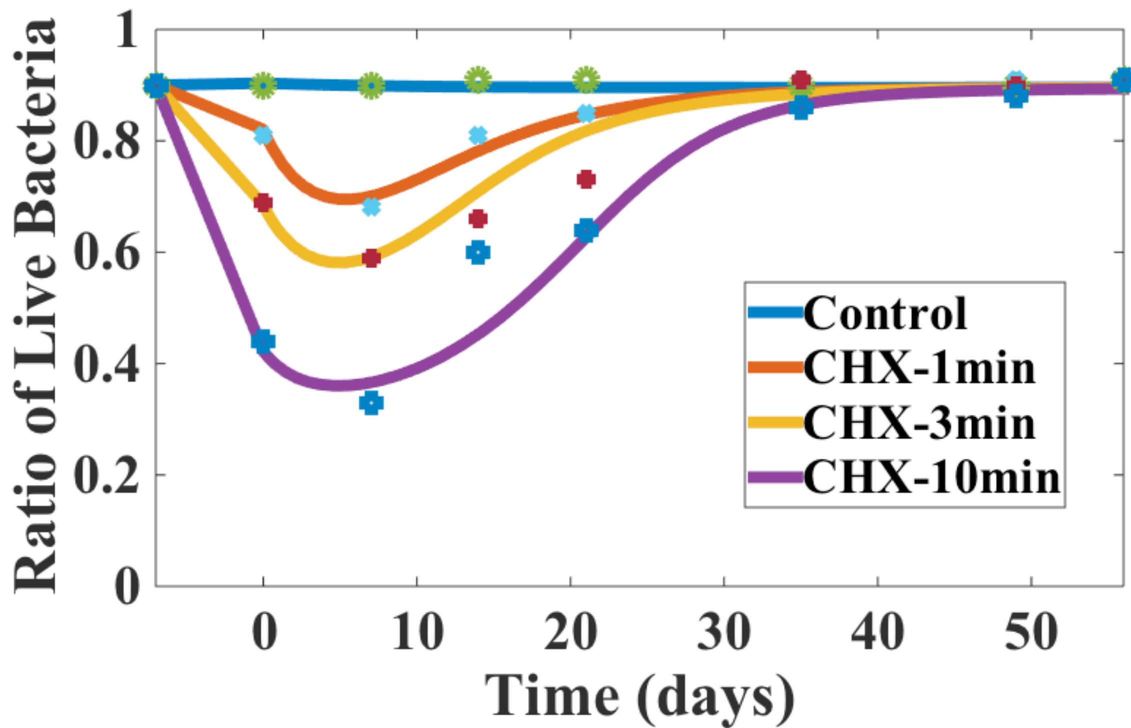

Table 1. The table for parameter values. Since there is no direct measurement of these parameters, we refer to their magnitude through published papers. All parameters with sources for order-of-magnitude are marked, otherwise, they are fitted with experiment results from[73] and[65], as well as from our experience.

Symbol	Description	Value	Unit	Reference
$c_0, H_{\max}, d_0, Q_{\max}$	Characteristic molecule concentration	8.24×10^{-3}	kg/m^3	1
c_2	Maximum growth rate for the susceptible	3×10^{-6}	s^{-1}	
c_3	Maximum death rate for the susceptible	6.5×10^{-2}	s^{-1}	
c_4	Maximum growth rate for the persister	3×10^{-7}	s^{-1}	
c_{12}	Maximum death rate for the persister	6×10^{-4}	s^{-1}	
c_5	Maximum EPS production rate	3.5×10^{-3}	s^{-1}	
c_7, c_8	Maximum nutrient consumption or antimicrobial consumption rate	1.0×10^{-7}	s^{-1}	
c_A	QS molecule production rate	6×10^{-7}	s^{-1}	
c_q	Growth factor production rate	1.0×10^{-5}	s^{-1}	
r_a	Decaying rate of effective antibiotics	1.0×10^{-6}	s^{-1}	
b_{sp}, b_{ps}	Conversion rate between the persister and the susceptible	1.5×10^{-7}	s^{-1}	7
r_{bs}	Natural death rate of susceptible bacteria	2.0×10^{-7}	s^{-1}	
r_{dp}	Dead bacteria recycling rate into EPS	2.2×10^{-6}	s^{-1}	
D_{pr}	Hinson constant	0.007		75
k_3	Monod constant	3.5×10^{-3}	kg/m^3	7
k_2, k_8	Monod constant	3.5×10^{-4}	kg/m^3	77
k_9	Monod constant	6.6×10^{-3}	kg/m^3	76
k_{12}	Monod constant	6.0×10^{-7}	kg/m^3	
k_Q	Monod constant	2.5×10^{-3}	kg/m^3	
$S_{\max}$	Carrying capacity for the susceptible bacteria	0.08		
$P_{\max}$	Carrying capacity for the persister bacteria	0.018		
$E_{\max}$	Carrying capacity for EPS	0.15		